

# Evidence for a fluid flow triggered spatio-temporal migration of seismicity in the 2001 $M_w$ 7.7 Bhuj earthquake region, Gujarat, India, during 2001–2013

PRANTIK MANDAL\*, MANISH KUMAR and KOUSHIK BISWAS

*CSIR – National Geophysical Research Institute, Uppal Road, Hyderabad 500 007, AP, India.*

*\*Corresponding author. e-mail: prantik@ngri.res.in*

We studied the variations in spatial and temporal clustering of earthquake activity (during 2001–2013) in the Kachchh seismic zone, Gujarat, India, by precisely relocating 3478 events using a joint hypocentral determination (JHD) relocation technique, and high-quality arrival times of 21032 P- and 20870 S-waves. Temporal disposition of estimated station corrections of P- and S-waves suggests that the fluid flow in the causative fault zone of the 2001 Bhuj mainshock increased during 2001–2010, while it reduced during 2011–2013, due to the healing process associated with the perturbed Kachchh fault zone. We also estimated the isotropic seismic diffusivities from epicentral growth patterns, which are found to be much lower than those observed for reservoir-induced seismicity sites in the world. Finally, we analysed the spatial and temporal evolution of this earthquake sequence by solving the diffusion equation of pore-pressure relaxation caused by co- and post-seismic stress changes associated with earthquakes. The value of the isotropic diffusivity is estimated to be  $100 \text{ m}^2/\text{s}$  for the Kachchh rift zone. This gives a higher permeability (after a lapse time of 14 years from the occurrence of the 2001 Bhuj mainshock) in comparison to those observed for other intraplate regions in the world. Our results suggest that the observed spatio-temporal migration of seismicity is consistent with the shallow (meteoric water circulation at 0–10 km depths) and deeper (metamorphic fluid and volatile  $\text{CO}_2$  circulation at 10–40 km depths) fluid flows in the permeable and fractured causative fault zone of the 2001 Bhuj earthquake.

## 1. Introduction

The determination of precise hypocentral locations of earthquakes is important in understanding the ongoing source processes in causative fault zones that can be achieved by delineating its geometry (Poupinet *et al.* 1984; Pujol 1988; Got *et al.* 1994). The precise relocations also allow us to map asperities and heterogeneities in the fault zone, which, in turn can pinpoint future locations of seismic failure, thereby, mitigating seismic hazards (Mandal and Horton 2007). One of the methods to obtain precise relocations of earthquakes is the joint hypocentral determination (JHD) technique,

which reduces location errors by incorporating station corrections of P- and S-waves (Pujol 1988). On 26 January 2001, a devastating earthquake of  $M_w$  7.7 occurred in Kachchh, Gujarat, claiming a death toll of 20,000 people. The aftershock activity of this earthquake is continuing even today, which is being monitored by the National Geophysical Research Institute, Hyderabad, with a neighbouring seismic network of 5–17 seismographs that provide an excellent aftershock dataset of the 2001 Bhuj earthquake. This includes 13  $M_w$  5.0–5.9, 250  $M_w$  4.0–4.9 and about 4000  $M_w$  3.0–3.9 events. To study the spatio-temporal changes in seismicity, first, we relocated earthquakes occurring in

**Keywords.** Fluid flow; migration of seismicity; relocations; rift zone; pore-pressure relaxation; seismic diffusivity.

the periods 2001–2005, 2006–2008, 2009–2010 and 2011–2013, using a JHD technique. Next, based on distributions of relocated hypocentres, we studied the spatio-temporal variations of seismicity in the Kachchh rift zone over the last 13 years, with an aim of improving our understanding of the seismogenesis of intraplate earthquakes occurring in this continental rift zone. We then analysed the station corrections to infer about the source processes in the causative fault zone of the 2001 mainshock.

The migration of static stress changes associated with the previously occurred 2001 Bhuj mainshock is found to be a key factor in triggering aftershocks in the region that are critically stressed (To *et al.* 2006; Mandal *et al.* 2007; Rastogi *et al.* 2013). However, the coseismic stress field can also be modified by other time-dependent processes like afterslip, viscoelastic relaxation of the lower crust and fluid flow, which in turn, controls the migration of seismicity (Antonoli *et al.* 2005). The modelling of diffusive processes of pore-pressure perturbation can explain successfully the migration of both tectonic and induced earthquakes (Nur and Booker 1972; Talwani and Acree 1984; Noir *et al.* 1997). The migration of seismicity observed during the 1997 Umbria–Marche (Italy) earthquake has been explained successfully through diffusion of a pore-pressure perturbation (generated by the coseismic stress changes associated with the mainshock) in a poro-elastic, fluid-saturated medium (Antonoli *et al.* 2005). In Kachchh, the occurrences of three earthquakes (*viz.*,  $M_w$  7.7 2001 mainshock, and  $M_w$  5.6 2005 and  $M_w$  4.9 2010 Kachchh events) have been related to the triggering through static stress changes (To *et al.* 2006; Mandal *et al.* 2007; Mandal 2009a). But, the seismicity pattern reveals that seismicity migrated to and activated both the Gedi and Allah–Bund faults in Kachchh, Gujarat, India, before the occurrences of impending mainshocks (Mandal *et al.* 2007; Mandal 2009a). Now, if we assume that the co- and post-seismic stress changes associated with the 2001 mainshock have promoted fluid flow in the aftershock zone, facilitating the migration of seismicity, then, it would be important to reinterpret the model of observed migration in Kachchh seismicity in terms of fluid flow and pore-pressure relaxation.

## 2. The 2001 Bhuj earthquake sequence

The 2001 Bhuj earthquake (figure 1) and its predecessor of comparable magnitude, which occurred in 1819, took place in the Kachchh Rift. The stresses associated with the rift system have changed from extensional to compressional, in response to the interplate deformation along the Himalaya during 20–40 Ma (Courillot *et al.* 1986;

Chung and Gao 1995). The  $M_w$  7.7 2001 Bhuj earthquake took place in the continental plate interior, away from the active plate boundaries like the Heart–Chaman plate boundary in the west ( $\sim 400$  km away) and the Himalayan plate boundary in the north ( $\sim 1000$  km away) (Gupta *et al.* 2001). This event occurred on a blind south dipping reverse fault and claimed a death toll of 20,000 people (Gupta *et al.* 2001). The 2001 Bhuj earthquake is of some special interest to seismologists worldwide because it represents a very compact source of large displacement and high-stress drop (Negishi *et al.* 2001; Antolik and Dreger 2003). A high-stress drop of 20 MPa over a small rupture area ( $20 \text{ km} \times 20 \text{ km}$ ) characterises the 2001 Bhuj mainshock (Negishi *et al.* 2001), and the *b*-value of the Bhuj earthquake sequence during 2001 is estimated to be  $\sim 0.88$  (Mandal *et al.* 2006). The last  $M_w$  4.3 aftershock occurred at 38 km depth on 8th March 2014, after thirteen years of the occurrence of the Bhuj mainshock. Analyses of the abundant data generated since 2001 have helped to image this rift and the seismogenic structures in great detail (Kayal *et al.* 2002; Mishra and Zhao 2003; Mandal and Pujol 2006; Mandal and Chadha 2008; Mandal and Pandey 2010; Mandal 2012). Presences of large-scale crustal intrusives and underplated magma at lower crustal levels have been delineated by local earthquake tomography and seismic refraction studies (Kayal *et al.* 2002; Sarkar *et al.* 2007; Mandal and Chadha 2008; Mandal and Pandey 2010). Recently, a joint inversion of P-receiver function and surface wave group velocity dispersion curves delineated a 4–6 km crustal as well as 6–12 km asthenospheric thinning beneath the Kachchh rift zone (Mandal 2012). Based on velocity structure and thermal modelling, Mandal and Pandey (2010) proposed that a compositionally highly altered lower crust (at 24–34 km depth) and a sub-crustal eclogitic layer (at 34–42 km depth) overlying a thin lithosphere ( $\sim 70$  km) characterise the Kachchh rift zone. They also suggested that the complex crust-mantle structure in the Kachchh rift zone might have resulted from the lithosphere and Deccan/Reunion mantle plume interaction at 65 Ma.

## 3. Geology and tectonics of Kachchh, Gujarat

The Kachchh basin is the earliest pericratonic rift basin formed in the western margin of the Indian plate during the Late Triassic break-up of the Gondwanaland (Biswas 1987, 2005). The rift evolution with the syn-rift sedimentation continued, through Jurassic till Early Cretaceous as the Indian plate separated from Africa and drifted northward,

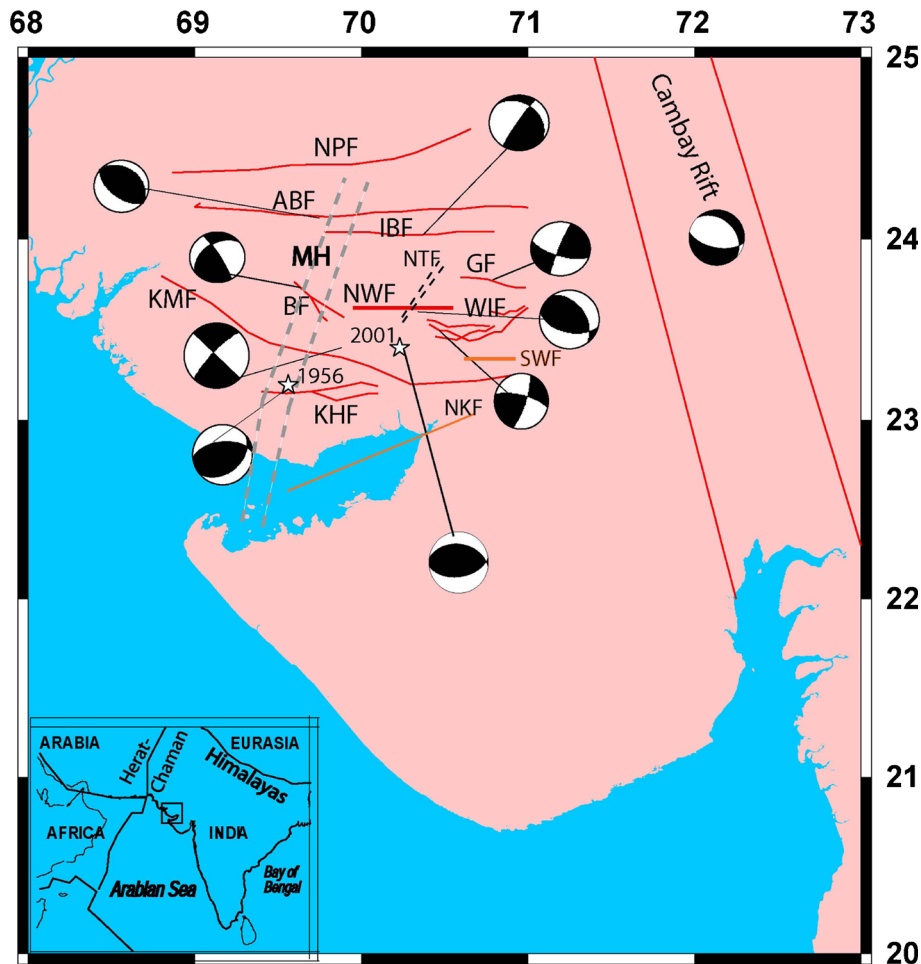


Figure 1. A plot showing major faults and associated available fault plane solutions in the Kachchh seismic zone, Gujarat, India. Locations (white stars) and focal mechanisms of the 2001 Bhuj and the 1956 Anjar earthquakes are also shown. Red lines represent the geologically mapped faults (Biswas 1987; Mandal *et al.* 2004). Major faults (marked by orange lines): Kachchh Mainland Fault (KMF); South Wagad Fault (SWF); North Kathiawar Fault (NKF); Katrol Hill Fault (KHF); Allah Bund Fault (ABF); North Wagad Fault (NWF); Nagar Parkar Fault (NPF); Gedi Fault (GF); Island Belt Fault (IBF); Wagad Imbricate Faults (WIF). Cambay rift zone is shown by thick parallel red lines while dotted grey lines mark the median high (MH). And, black dotted lines represent the inferred north dipping transverse fault (Mandal and Pandey 2010). The inset is showing the key map for the area with reference to Indian plate boundaries (dark lines).

along an anticlockwise path. The E–W trending rift basin is bound by the Nagar Parkar uplift on the north, the Kathiawar uplift on the south along sub-vertical Nagar Parkar Fault (NPF) and North Kathiawar Fault (NKF) (figure 1, Biswas 1987). This rift zone is characterised by three intra-rift faults, the Island Belt Fault (IBF), the Kachchh Mainland Fault (KMF), and the South Wagad Fault (SWF), with intervening grabens and half-grabens. Tilted blocks and half-grabens style the structure within the south tilted asymmetric Kachchh rift basin. The NKF is the bounding master fault along which the rift subsided most. All the faults are sub-vertical dipping  $90^{\circ}$ – $75^{\circ}$  towards the adjacent half-graben or graben (Biswas 1987). In the western part, the step-faulted uplifts are tilted to the south with flexures draped over the faulted up northern edges (Biswas 2005). In the eastern part, a large uplift – the Wagad uplift, occurs between the KMF

and IBF. It is tilted opposite to the north with a narrow deformation zone along the faulted southern edge (Biswas 2005). An imbricate fault system characterises the Wagad uplift (figure 1). SWF is the eastward continuation of KMF after side stepping with an overlap zone between Bhachau and Adhoi. Another important tectonic feature in the Kachchh rift zone is a subsurface basement ridge – Median High (MH) that crosses the basin at a right angle to its axis in the middle. Acting as a hinge, it divides the basin into a deeper western part and a shallower and more tectonised eastern part (figure 1, Biswas 1987). We can also observe that the rift is terminated in the east against a transverse subsurface basement ridge (i.e., the Radhanpur Arch). This arch is the western shoulder of the adjacent N–S oriented extensional Cambay rift (figure 1). To the west, the rift merges with the offshore shelf (Biswas 1987).

During the present compressive stage, the Radhanpur arch acts as a stress barrier (a large-scale heterogeneity/asperity that dampens the stress propagation) for eastward movements along the principal deformation zones, which is creating additional strain between the arch and the Median High (Biswas 2005). Towards the eastern end of the Mainland uplift, the right lateral Kachchh Mainland Fault (KMF) becomes the south Wagad Fault (SWF) by left stepping with an overlap in the region between Samakhali and Lakadiya (Biswas 2005). This overstep zone, formed initially as Samakhali–Lakadiya graben, is presently a convergent transfer zone undergoing transpressional stress. Expectedly, this is the most favoured site for rupture nucleation, which gets further support from the occurrences of closely spaced epicentres of two major earthquakes – 1956 Anjar ( $M_w$  6.0) and 2001 Bhuj ( $M_w$  7.7) – in this zone, and concentration of aftershocks around it.

The aftershock data suggests a reverse slip on a fault plane dipping  $40^\circ$ – $60^\circ$  south as the causative fault for repeated earthquake nucleation (Mandal and Horton 2007). Continued stress and repeated thrusting generate fractures related to the main fault forming a highly stressed fault zone, which seems to be the zone of repeated earthquake nucleation (Biswas 2005). This earthquake nucleation zone is defined by several subsidiary faults branching off the main SWF. The causative fault, the NWF (north Wagad Fault), of the Bhuj 2001 earthquake seems to occur on a fault that extended westward as a branch of SWF (Biswas 2005). Large intraplate stress perturbations associated with the pre-existing fault intersection, favourably oriented maximum horizontal stress direction and mafic crustal intrusive bodies below the Kachchh rift zone are shown to be the causative for the generation of the 2001 Bhuj earthquake (Gangopadhyay and Talwani 2003; Mandal and Pandey 2010). The presence of a fault intersection (between NWF and north dipping transverse fault (NTF) (figure 1)) in the 14–24 km depth range appears to lead to large stress concentrations in the lower-crustal magmatic layer (at 14–34 km depth), thereby becoming the favoured zone of earthquake nucleation (Mandal and Pandey 2010). Further, the fluid released by the metamorphism of lower crustal rocks aids the slippage along this causative fault, resulting in the occurrences of the 2001 Bhuj earthquake sequence (Mandal and Pandey 2010; Mandal 2012).

#### 4. Local seismic network and data

Through a homogeneously distributed local seismic network consisting of 5–12 digital seismographs

equipped with GPS timing system, the National Geophysical Research Institute (NGRI), Hyderabad, has been monitoring the aftershock activity of the 2001  $M_w$  7.7 Bhuj earthquake, since February 4, 2001. In addition, for our present study, we have also used data from the 16 seismic stations from the CERI network, Memphis (13–21 February, 2001) and seismic stations of the Hirosaki University, Japan (28 February–7 March, 2001). Thus, P- and S-arrival times from a total of 58 stations were used for the tomographic inversion during 2001–2005, resulting in a homogeneous coverage of the aftershock zone. To further strengthen this network, 20 strong motion accelerographs (equipped with GPS timing system) were also deployed in the epicentral zone, during 2002–2006 (marked by open grey triangles, figure 2a, d, g, j). P- and S-arrivals were also used from the accelerographs for locating strong earthquakes of moment magnitude ( $M_w$ ) exceeding 2.8. During 2001–2013, some seismograph/accelerograph station locations were shifted, which led to a total of 42 sites. This setup of seismic stations resulted in a total of 42, 19, 12 and 11 seismic stations during the periods 2001–2005, 2006–2008, 2009–2010 and 2011–2013, respectively. We noticed that 6–8 seismograph stations (marked by filled grey triangles in figure 2a, d, g, j) covering the aftershock zone (sampling the same crustal volume) have been present for the time periods 2001–2005, 2006–2008, 2009–2010, and 2011–2013, which enabled us to study the variations in relocations of aftershocks in the Kachchh seismic zone. Most of these stations were installed on hard Jurassic sediments and hence have a good signal-to-noise ratio. The distance between station and epicentres vary from 14 to 90 km. This network resulted in an azimuthal gap of less than  $180^\circ$ . Most of these stations were installed on hard Jurassic sediments, and hence have a good signal-to-noise ratio, so as to read the arrival time of P phase within 0.05 s. S phase picks have larger errors than P-wave picks. Since NGRI stations are closely spaced in the epicentral zone, at least one station was always within the distance of the hypocentral depth resulting in good, accurate S picks, which led to a good control on focal depth estimation (i.e.,  $\pm 1$  km).

## 5. Methodology

### 5.1 Joint hypocentral determination (JHD) relocations of earthquakes

Initial earthquake locations for the time periods (2001–2005, 2006–2008, 2009–2010 and 2011–2013) were obtained using the routine earthquake location code inbuilt in the SEISAN software (Havskov and

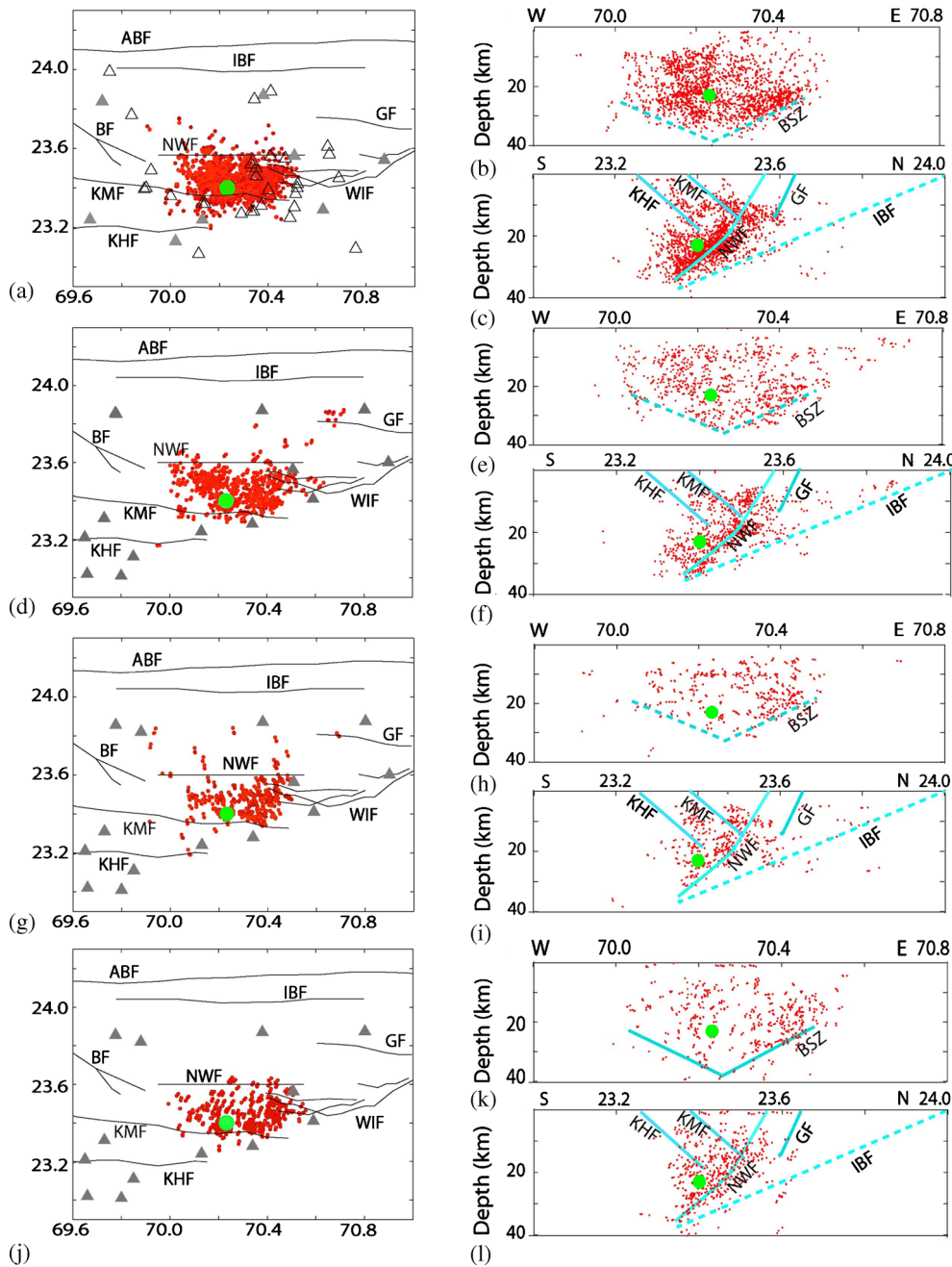


Figure 2. Precise JHD relocations of earthquakes in the Kachchh seismic zone. (a) Epicentres of relocated events during 2001–2005, (b) N–S depth sections of relocated events during 2001–2005, (c) E–W depth sections of relocated events during 2001–2005. (d–f), (g–i) and (j–l) represent the same plots as (a–c) for relocated events during 2006–2008, 2009–2010 and 2011–2013, respectively. Small open circles mark the relocated events with magnitudes of  $M_w$  2.0–5.8 while a large solid circle marks the 2001 Bhuj mainshock. The distribution and names of the faults are same as shown in figure 1. BSZ marks the base of the seismogenic zone (pink dotted lines). Grey lines mark the geometry of seismically active fault zones. Open grey triangles mark the seismograph stations.

Ottmoller 2003) and the one-dimensional crustal velocity model of Mandal (2007). The grouping of earthquakes into four different time periods during 2001–2013 have been done by considering bursts of seismicity with the mainshock of  $M_w \geq 4.9$  as separate groups (Rodkin and Mandal 2012). The average location rms is 0.03 s. The mean errors in horizontal and vertical estimates of earthquake location are 1.5 and 2.5 km, respectively.

These initial earthquake locations are relocated using the JHD technique (Pujol 1988) and the above-discussed 1-D velocity structure (Mandal 2007). For JHD, the  $V_p/V_s$  ratio is fixed at 2.5 for the upper sedimentary layer (0–2 km depth) (Mandal *et al.* 2006), whereas, for other crustal layers (2–40 km depth), the  $V_p/V_s$  ratio is fixed at 1.73. First, the JHD technique (Pujol 1988) was being applied on four datasets of P- and S-arrivals from

initially SEISAN located earthquakes (table 1). These events were recorded from 5–18 stations during 2001–2005, 2006–2008, 2009–2010 and 2011–2013, to obtain precise, accurate earthquake relocations. The JHD relocations of earthquakes (figure 2) clearly delineate two sharp E–W trending source zones in the Kachchh seismic zone. One is along the NWF and another is associated with the GF. With the help of JHD relocation method, the mean uncertainty in epicentral location is reduced from 1500 to 500 m while the focal depth uncertainty is reduced from 2500 to 1000 m. These precisely relocated hypocentres clearly demarcate the geometry of seismically active fault zones in the KSZ like NWF, GF, KHF, NTF and KMF (figure 2).

The distribution of relocated hypocentres during 2001–2005 shows that most of the events are clustered within an E–W trending crustal volume below the main rupture zone of the 2001 Bhuj mainshock. This extends 55 km N–S (from latitude 23.25° to 23.75°N), 45 km E–W (from longitude 70.0° to 70.55°E) and 35 km in depth (from 1 to 36 km) (figure 2a). Fewer events are also clustered along the Gedi Fault (GF) while some scattered events are located along the ABF and IBF (figure 2a). The N–S hypocentral depth distribution of earthquakes suggests a marked concentration along the south dipping NWF (i.e., the north Wagad Fault) (figure 2b), reaching the ground surface at Burudia village (~23.6°N) and it extends along the Wagad uplift (figure 2a). Our result gets further support from the presence of initial fault movement as evidenced from the geological trenching data of McCaIpin and Thakkar (2003). The E–W cross section shows a marked change (~10–15 km) in seismogenic depth across the main rupture zone of the 2001 Bhuj mainshock (figure 2c). This change in seismogenic depth could be attributed to the lateral variation in maficness across the main rupture zone (Mandal and Pandey 2010). The patterns of hypocentral distributions remain the same, except a northward extension of the aftershock zone during 2006–2010 (figure 2d–i);

however, a similar pattern of hypocentral distribution as observed during 2001–2005 (figure 2a–c) is also noticed during 2011–2013 with relatively fewer number of events (figure 2j–l). The relocated hypocentres very clearly delineate the north dipping KMF, KHF and NTF, south dipping NWF, and almost vertical GF (figure 2). The geometries of our delineated faults are in good agreement with the geologically mapped faults in the region (Biswas 2005).

## 5.2 Station corrections

The P- and S-station corrections were also estimated from the JHD relocation of earthquakes (Pujol 1988). The estimated station corrections for P-wave varied from –0.62 to +1.03 s during 2001–2005, –1.04 to +0.12 s during 2006–2008, –0.97 to +0.09 s during 2009–2010 and –0.21 to +0.89 s during 2011–2013 (figure 3a–h). On the other hand, the estimated station corrections for S-wave varied from –2.66 to +0.44 s during 2001–2005, –1.98 to +0.12 s during 2006–2008, –1.91 to +0.32 s during 2009–2010 and –0.39 to +0.94 s during 2011–2013 (figure 3a–h). The estimated average standard deviation for P and S wave station corrections were found to be 0.11, 0.25, 0.17 and 0.10, for the periods 2001–2005, 2006–2008, 2009–2010, and 2011–2013, respectively. Now, we know that a positive (negative) station correction indicates that the observed travel time is longer (shorter) than that calculated from a given velocity model, suggesting that the actual velocity structure is lower (higher) than the given velocity model used in the earthquake location. During 2001–2005, the aftershock zone is observed to be mainly characterised by large positive P-corrections and smaller negative S-corrections, thus, the central aftershock zone shows relatively markedly slower P velocity and relatively slower S velocity in comparison to surrounding regions (figure 3a–h). During 2006–2008 and 2009–2010, smaller negative P- and S-corrections (relatively slower velocities) characterise the aftershock zone while larger negative P- and S-corrections characterise the surrounding regions (faster velocities). During 2011–2013, we observed that larger positive P- and S-corrections (relatively slower velocities) characterise the central aftershock zone while the surrounding regions are dominated by smaller positive corrections (relatively faster velocities). We also noticed consistent smaller-to-large positive corrections (slower velocities) in the south-eastern region of the Bhuj mainshock, where Deccan basalts are found to be exposed. This pattern of changes in station corrections of P- and S-waves suggests that the P- and S-corrections

Table 1. *Input data used for the JHD relocation study.*

| Dataset | Period of recording | No. of earthquakes, |                       | No. of P- arrivals | No. of S- arrivals |
|---------|---------------------|---------------------|-----------------------|--------------------|--------------------|
|         |                     | relocated by JHD    | Total no. of stations |                    |                    |
| 1       | 2001–2005           | 1888                | 42                    | 10988              | 10964              |
| 2       | 2006–2008           | 706                 | 19                    | 4930               | 4922               |
| 3       | 2009–2010           | 477                 | 12                    | 2551               | 2545               |
| 4       | 2011–2013           | 1655                | 11                    | 10253              | 10135              |

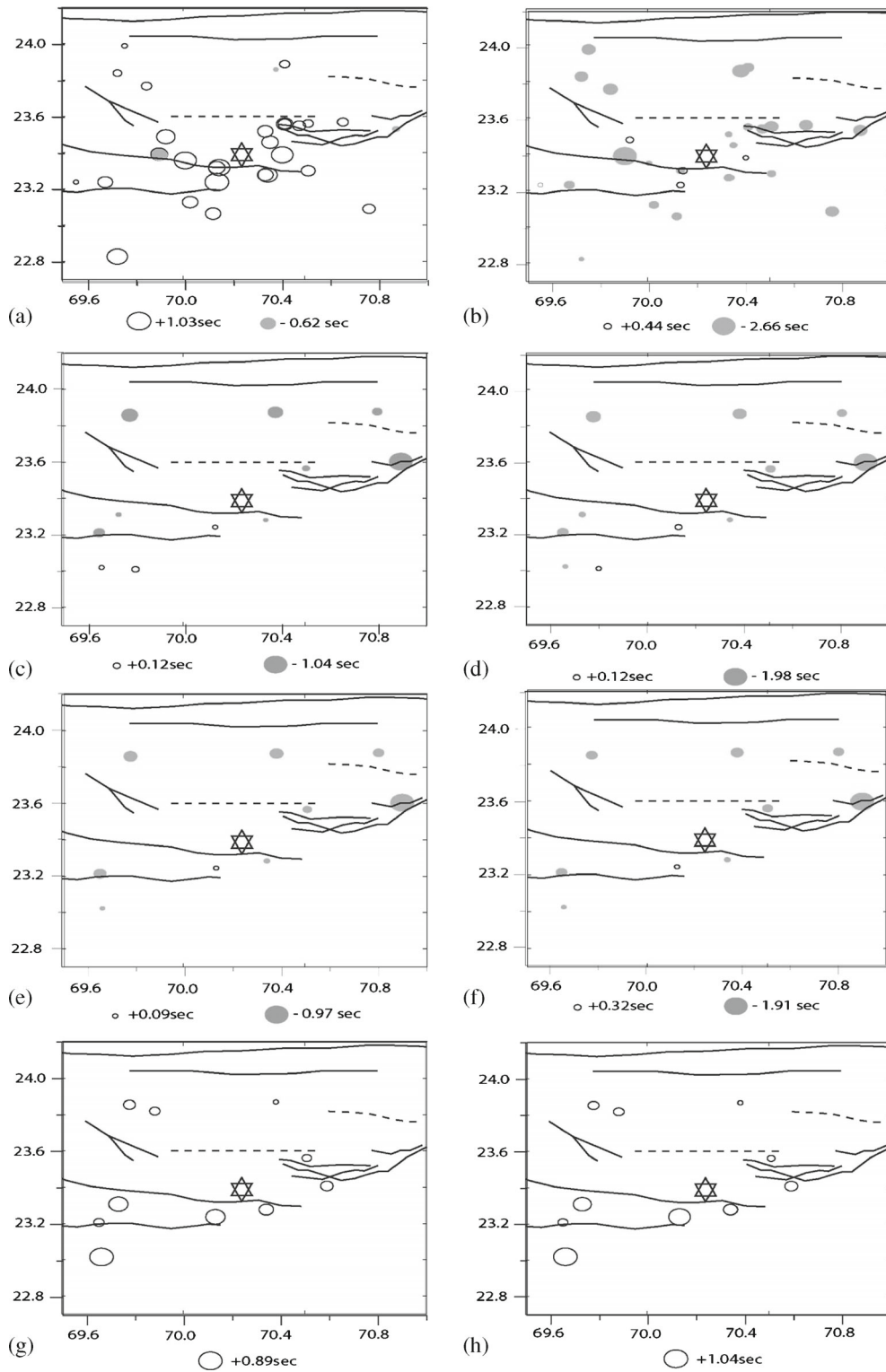


Figure 3. Estimated station corrections from JHD of events during 2001–2005, (a) for P-waves and (b) for S-waves. While (c–d), (e–f) and (g–h) represent the same plots as (a–b) for relocated events during 2006–2008, 2009–2010 and 2011–2013, respectively. Star symbol marks the location of the 2001 mainshock. Open and solid circles denote positive and negative station corrections, respectively. The sizes of circles represent the magnitude of station corrections. The distribution and names of the faults are same as shown in figure 1.

became more negative (faster velocities) in the causative fault zone of the 2001 Bhuj earthquake over the passage of time during 2001–2013

(figure 3a–h). Using estimated P- and S-corrections, we also measured  $V_p/V_s$  values for four different periods (figure 4a–d), which suggested an increase

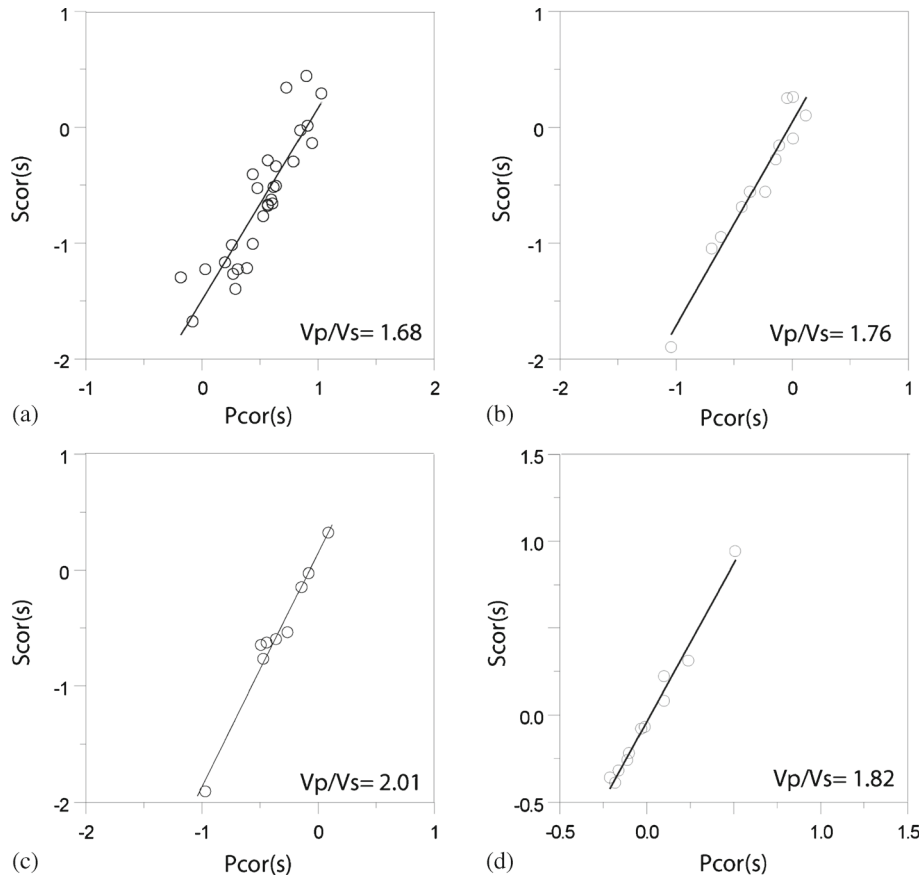


Figure 4. Plot of estimated JHD station corrections for P- (Pcor in s) and S- (Scor in s) waves for different time periods (a) 2001–2005, (b) 2006–2008, (c) 2009–2010, and (d) 2011–2013.

in  $V_p/V_s$  values during 2001–2010, while these values decrease during 2011–2013. Thus, estimated station corrections and  $V_p/V_s$  values apparently suggest that during 2001–2010, there were more fluid flows in the damaged MRZ immediate after the occurrence of the 2001 Bhuj MS. However, subsequently they show relatively faster velocities in the MRZ during 2011–2013, that could probably be related to the healing process (closing of cracks thereby lower pore fluid pressure) of the 2001 Bhuj earthquake.

## 6. Temporal changes in the growth of aftershock zone in space and time

From table 2, we notice that the linear growth of the epicentral zone increases during 2001–2010 and attains its maximum of 7200 km<sup>2</sup> during 2009–2010 and decreases to 5454 km<sup>2</sup> during 2011–2013 (figure 5). In the same line, we also notice that growth in the hypocentral zone of the 2001 Bhuj earthquake sequence suggests more expansion in E–W direction than in N–S direction (figure 5b, c). This growth in E–W direction also attains a maximum of 4089 km<sup>2</sup> during 2009–2010, but it reaches

Table 2. *Epicentral growth in the Kachchh seismic zone during 2001–2013.*

| Year      | Area of the epicentral zone | Time period (days) | Seismic diffusivity (m <sup>2</sup> /s) |
|-----------|-----------------------------|--------------------|-----------------------------------------|
| 2001–2005 | 83 × 47 km <sup>2</sup>     | 1790               | 25.22                                   |
| 2006–2008 | 67 × 102 km <sup>2</sup>    | 1095               | 75.55                                   |
| 2009–2010 | 80 × 90 km <sup>2</sup>     | 730                | 119.4                                   |
| 2011–2013 | 101 × 54 km <sup>2</sup>    | 1095               | 57.65                                   |

its maximum of 2440 km<sup>2</sup> in the N–S direction, during 2001–2005.

It is well established that linear growth of the epicentral area with time suggests a relationship in the form of  $L^2 \sim t$ . It implies  $L^2/t = \alpha_s$ , a proportionality constant termed as seismic hydraulic diffusivity by Talwani and Acree (1984/85). Thus, the seismic diffusivity for different time periods can be estimated based on the growth of epicentral area ( $L^2$ ), which are estimated to be 3901 km<sup>2</sup> during 2001–2005, 1467 km<sup>2</sup> during 2006–2008, 183 km<sup>2</sup> during 2009–2010 and 873 km<sup>2</sup> during 2011–2013, respectively (table 2). The seismic diffusivity values ( $\alpha_s$ ) for different time periods in the



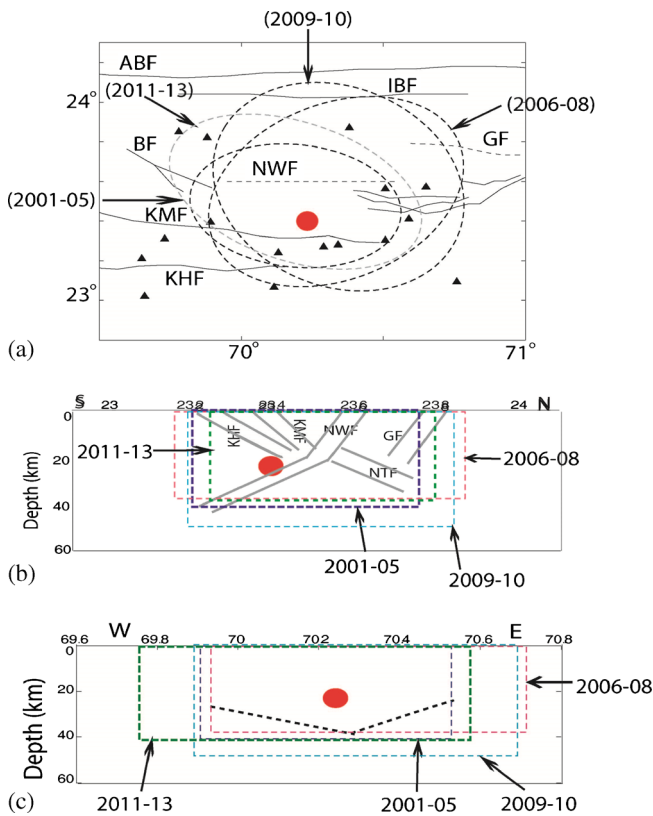


Figure 5. (a) Temporal variations in epicentral growth (marked by dotted lines) in the Kachchh seismic zone during 2001–2005, 2006–2008, 2009–2010 and 2011–2013, respectively. A solid red circle marks the 2001 mainshock. (b) Temporal variations in hypocentral zone growth (marked by dotted lines) in the E–W direction during 2001–2005 (violet), 2006–2008 (pink), 2009–2010 (blue) and 2011–2013 (green), respectively, and (c) temporal variations in hypocentral zone growth in the N–S direction during 2001–2005 (violet), 2006–2008 (pink), 2009–2010 (blue) and 2011–2013 (green), respectively.

Kachchh seismic zone (KSZ) are calculated to be  $25.22 \text{ m}^2/\text{s}$  during 2001–2005,  $15.51 \text{ m}^2/\text{s}$  during 2006–2008,  $2.90 \text{ m}^2/\text{s}$  during 2009–2010 and  $9.23 \text{ m}^2/\text{s}$  during 2011–2013, respectively (table 2). On an average, the seismic diffusivity in the KSZ during 2001–2013 reduces from  $25.22$  (during 2001–2005) to  $2.90 \text{ m}^2/\text{s}$  (during 2010–2011), and then it again increases to  $9.23 \text{ m}^2/\text{s}$  during 2011–2013.

From table 2, we can infer that the occurrence of the 2001 Bhuj mainshock might have resulted in numerous fractures in the main rupture zone, which might have facilitated the fluid flow in the aftershock zone resulting in larger epicentral growth and seismic diffusivity values during 2001–2008. We also observe a marked reduction in epicentral growth and seismic diffusivity during 2010–2011, which could be related to the healing process of the main rupture zone. Most interestingly, we notice an increase in both epicentral growth and seismic diffusivity during 2011–2013, this is certainly related to the re-activation

of neighbouring faults resulting in migration of seismic activity.

Note that the above estimates of isotropic diffusivity using the epicentral zone might be quite underestimated because of the fact that we have not considered the anisotropy. In fact, the occurrences of earthquakes involve a volume ( $x$ ,  $y$  and  $z$ ), thus, for calculating robust estimates of diffusivity one needs to consider changes in all three directions. Thus, actual estimates of anisotropic diffusivity for the Kachchh region could be higher than  $2.90\text{--}25.22 \text{ m}^2/\text{s}$ .

### 6.1 Estimation of seismic diffusivity

The seismic hydraulic diffusivity is explained using the solution of a pore-pressure diffusion problem. Here, we assume that, first, the diffusion process of pore-pressure relaxation is generated by coseismic-stress changes as a pressure perturbation, and it propagates through a fluid-saturated medium. One needs to solve Darcy’s equation for the modelling of pore-pressure relaxation for explaining the migration of seismicity. The Darcy’s law in an isotropic and homogeneous poroelastic fluid-saturated medium can be written as:

$$\partial p/\partial t = \partial/\partial x[\alpha(\partial p/\partial x)], \quad (1)$$

where  $t$  is the measured time from the origin time of the mainshock,  $p$  is the pressure,  $x$  is any observation point in the medium and  $\alpha$  is the hydraulic diffusivity tensor of the material in which diffusion takes place. Further, the hydraulic diffusivity tensor ( $\alpha$ ) and permeability tensor ( $K$ ) can be related through the following relation:

$$\alpha = K/\varepsilon\nu C_T, \quad (2)$$

where  $\varepsilon$  and  $\nu$  are the rock porosity and fluid viscosity, respectively.  $C_T$  represents the coefficient of the isothermal compressibility.

For a step-function point-source pore-pressure in a homogeneous fluid-saturated medium, the solution of equation (1) can be written as (Shapiro *et al.* 1999, 2003):

$$r = (4\pi\alpha t)^{1/2}, \quad (3)$$

where  $t$  is the time of injection or nucleation of triggering front.  $\alpha$  is a scalar diffusivity and  $r$  is the radius of triggering front.

According to the above-described procedure, first the pore-pressure change reaches a point  $r$  at time  $t$ , and then it triggers an event. Thus, the fluid flow may trigger an earthquake at a location  $r$  at any time  $t$  after the pore-pressure perturbation. Therefore, in an  $(r, t)$  plot, seismicity should lie below the parabola defined by equation (3) (Shapiro *et al.* 2003). In this method, the distances

between hypocentres are measured, thus considering that pore-pressure relaxation begins at the origin time and at the hypocentre of the causative shock.

### 6.2 Application to the 2001 Bhuj earthquake sequence

Figure 6(a) shows the temporal distribution of aftershock activity during 2001–2013 with several

bursts of seismic activity associated with moderate size earthquakes, which is being generated using a catalogue of  $M_w \geq 3.0$  Bhuj aftershocks. We use this catalogue for our study, because of the fact that earlier researchers have shown a cut-off magnitude of 3.0 for the Bhuj earthquake catalogue through the frequency–magnitude (G–R) distribution (Mandal et al. 2006; Rodkin and Mandal 2012). These bursts of activity are being attributed

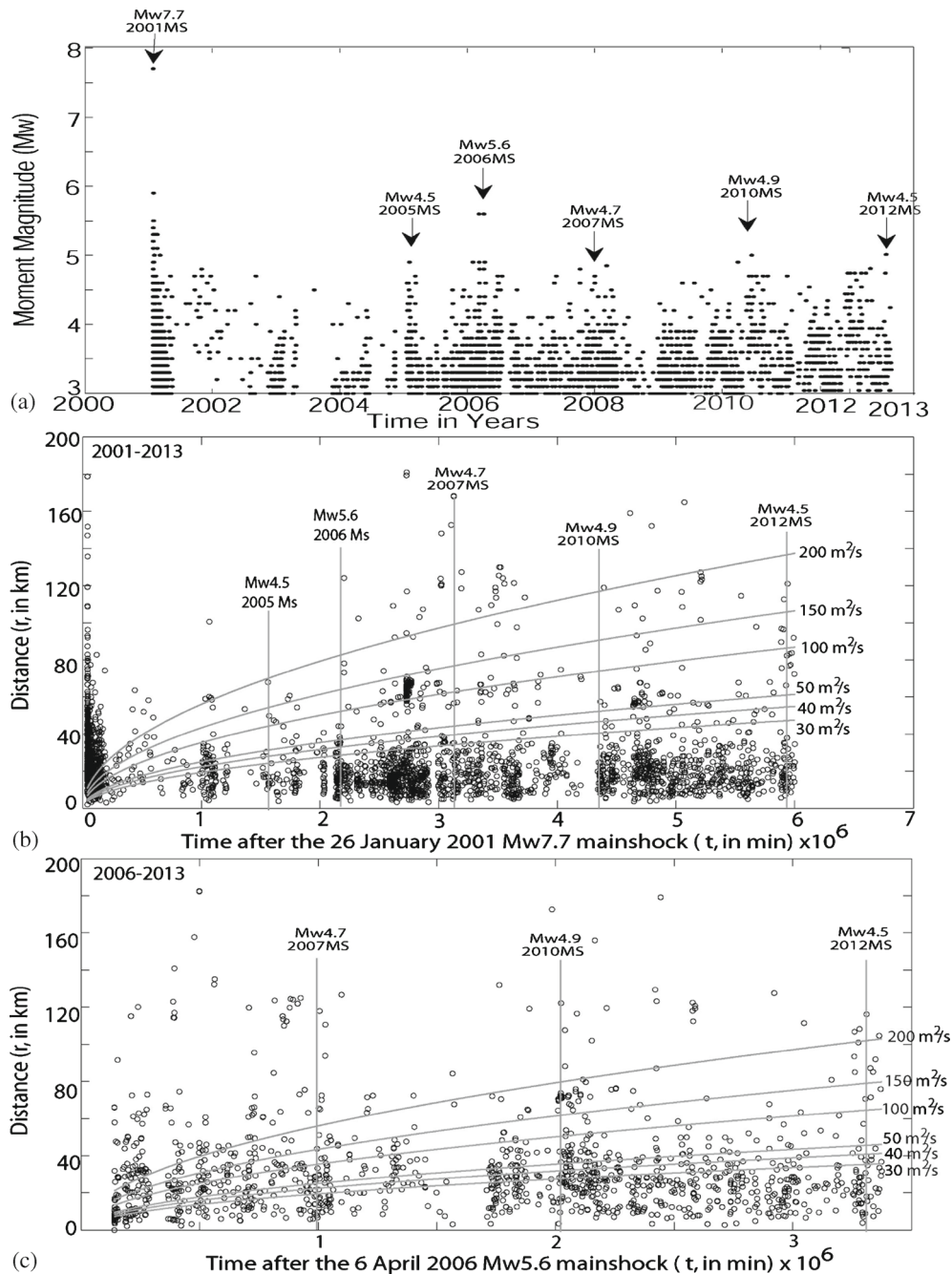


Figure 6. (a) Temporal distribution of the Kachchh seismicity during 2001–2013 showing bursts of seismic activity, which could be related to circulation of deep metamorphic fluids, (b) A  $(r, t)$  plot showing spatio-temporal distribution of earthquakes, wherein position and origin time are plotted in distance  $(r)$  versus time  $(t)$ . The predicted triggering front from equation (3) is marked by the thick black lines assuming three different anisotropic diffusivity values (i.e.,  $D = 30, 40, 50, 100, 150$  and  $200 \text{ m}^2/\text{s}$ ). The grey lines indicate the occurrences of significant events. (c) Similar  $(r, t)$  plot for the 6 April 2006 event ( $M_w 5.6$ ). The grey lines indicate the occurrences of significant events.

to the circulation of deep metamorphic fluids and volatile CO<sub>2</sub> in the causative fault zone (i.e., NWF) of the 2001 Bhuj mainshock (Rodkin and Mandal 2012).

The  $(r, t)$  plots shown in figure 6(b, c) are constructed using the above catalogue of  $M_w \geq 3.0$  Bhuj aftershocks. We also plotted in figure 6(b, c), the triggering front defined by equation (3) for different values of isotropic diffusivity ( $\alpha$ ) and the 2001 Bhuj spatio-temporal aftershock distribution. Aftershock locations  $r$  and origin times  $t$  are plotted starting from the 26 January 2001 (08:55 UTC  $M_w$  7.7) Bhuj event. Figure 6(b) shows that almost 80% of the seismicity distributions (during 2001–2013) lies below the triggering front parabola as predicted by the equation (3) for an isotropic diffusivity value of 100 m<sup>2</sup>/s. While almost 95%, 90% and 85% of the aftershock activity lies below the triggering front parabola as predicted by the equation (3) for the isotropic diffusivity values of 200, 150 and 100 m<sup>2</sup>/s, respectively (figure 6b). We have also drawn similar  $(r, t)$  plot for aftershock activity associated with the moderate size event of 6 April 2006 ( $M_w$  5.6) (figure 6c). We notice from figure 5(c) that almost 90% of the seismicity associated with the 6 April 2006 event on the Gedi Fault (23.7°N, 70.7°E) lies below the triggering front parabola as predicted by equation (3) for an isotropic diffusivity value of 100 m<sup>2</sup>/s (figure 6c). However, we also notice from figure 6(b, c) that a distinct clustering of aftershock activity associated with the 6 April 2006 event lies below the predicted parabola for an isotropic diffusivity of 100 m<sup>2</sup>/s. Thus, we infer that the isotropic seismic diffusivity for the Kachchh seismic zone is 100 m<sup>2</sup>/s, which explains the 85% seismicity associated with the 2001 Bhuj earthquake sequence during 2001–2013.

## 7. Discussions and conclusions

In this paper, we model the spatial and temporal evolution (2001–2013) of seismicity during the 2001 Bhuj earthquake sequence in terms of subsequent failures promoted by fluid flow. First, we estimate the precise relocations of aftershocks for time periods 2001–2005, 2006–2008, 2009–2010, and 2011–2013 by estimating station corrections for P- and S-waves through the joint hypocentral determination relocation technique. Since, the temporal distribution of the 2001 Bhuj earthquake sequence (figure 6a) shows epochs of substantial increase in seismic activity during the periods 2001–2005 (with  $M_w$  7.7), 2006–2008 (with  $M_w$  5.6), 2009–2010 (with  $M_w$  4.9), and 2011–2013 (with  $M_w$  5.0), we grouped events coinciding with these epochs

of substantial increase in seismic activity with MS of  $M_w \geq 4.9$  (figure 6a). The precise, accurate relocations of events led to the delineation of seismically active fault zones in the KSZ, viz., south-dipping NWF and GF and north dipping KMF and NTF. These relocations clearly delineate a fault intersection between NWF and NTF at 15–25 km depth range, where the 2001 mainshock took place. The P-wave station corrections vary from  $-0.62$  to  $+1.03$  s during 2001–2005,  $-1.04$  to  $+0.12$  s during 2006–2008,  $-0.97$  to  $+0.09$  s during 2009–2010 and  $-0.21$  to  $+0.89$  s during 2011–2013, while those for S-waves range from  $-2.66$  to  $+0.44$  s during 2001–2005,  $-1.98$  to  $+0.12$  s during 2006–2008,  $-1.91$  to  $+0.32$  s during 2009–2010 and  $-0.39$  to  $+0.94$  s during 2011–2013. The temporal disposition of estimated station corrections of P- and S- waves, which suggests that the fluid flow in the causative fault zone of the 2001 Bhuj mainshock has increased during 2001–2010, while it reduced during 2011–2013 due to the healing process associated with the perturbed Kachchh fault zone. In the main rupture zone (at 10–35 km depths), crack/fracture density increases over the passage of time (during 2001–2010) because of the intense fracturing that occurred both during the mainshock and post-seismic periods, but, the rupturing process and fluid flow within the fault zone has been observed to be reduced during 2011–2013, which could be related to the healing process associated with the perturbed Kachchh rift zone.

Using these precise relocations of earthquakes, we estimate the isotropic seismic diffusivity values from the epicentral growth in the KSZ during 2001–2005, 2006–2008, 2009–2010 and 2011–2013, which range between 2.90 and 25.22 m<sup>2</sup>/s. Our results show larger epicentral growth and seismic diffusivity values during 2001–2008, which could be attributed to the more fluid flow in the fractured and damaged main rupture zone caused by the occurrence of the 2001 mainshock. On the other hand, we observe a marked reduction in epicentral growth and seismic diffusivity during 2010–2011, which could be related to the healing process of the main rupture zone. Most interestingly, we notice an increase in both epicentral growth and seismic diffusivity during 2011–2013, which could be related to the re-activation of neighbouring faults (probably related to post-seismic static stress transfer phenomena) resulting in migration of seismic activity.

Finally, in this paper, we model the diffusion process of pore-pressure relaxation as a pressure perturbation generated by post-seismic stress changes, which then propagates through a fluid-saturated medium. Our modelling suggests an isotropic diffusivity of 100 m<sup>2</sup>/s, which explains the

aftershock activity in the KSZ during 2001–2013. The higher value of observed isotropic diffusivity can be explained by the fact that the main aftershock zone of the 2001 Bhuj mainshock is characterised by the relatively higher permeability than surrounding regions.

The inferred isotropic hydraulic diffusivities for different seismically active regions of the world range from  $10^{-2}$  to  $10^4$  m<sup>2</sup>/s (Noir *et al.* 1997; Shapiro *et al.* 1999; Talwani and Acree 1984). An isotropic diffusivity of 100 m<sup>2</sup>/s for the KSZ gives a permeability value of  $1.45 \times 10^{-11}$  m<sup>2</sup> [by using equation (2) and assuming  $C_t = 2.9 \times 10^{-9}$  Pa<sup>-1</sup>,  $\nu = 10^{-3}$  Pa.s, and  $\varepsilon = 0.05$  (Miller *et al.* 2004)]. This value is similar to the permeability values ( $\sim 5 \times 10^{-11}$  m<sup>2</sup> or more) obtained by Miller *et al.* (2004) for the 1997 northern Italian earthquake region, for a fluid-connected pulse propagation depth of 10 km and a pulse time duration of one month. However, our estimated permeability value is larger than the effective background permeability ( $k \approx 10^{-13}$  m<sup>2</sup>) found by Rodkin and Mandal (2012) in the same area. Now, we know that the permeability value can be of the order of  $10^{-17}$  to  $10^{-14}$  m<sup>2</sup> in the upper crust while it can be reduced to  $10^{-18}$  m<sup>2</sup> in the presence of metamorphic fluids in the lower crust (Manning and Ingebritsen 1999). Only at subsurface conditions, the crustal permeability values can increase up to  $10^{-15}$ – $10^{-13}$  m<sup>2</sup> (Gudmundsson 2000). Thus, our estimated permeability of  $7.25 \times 10^{-12}$  m<sup>2</sup> for the KSZ, suggests prevailing conducive conditions for deeper fluid circulation in the lower crust below the study area.

In the same line of support, we notice from figure 2 that aftershocks are not substantially confined to the causative fault of 2001 Bhuj mainshock, rather, they show a larger concentration within the adjacent crustal block above the causative fault than that adjacent to it from below. It is already established that this kind of aftershock pattern is typical of strong earthquakes, which suggests the possibility of diffusion of fluids in the aftershock zone (Gliko 2011). Even for the bursts of seismic activity in 2006 and 2010, the activity was not confined to the main causative fault of the 2001 mainshock. This suggests that after a lapse of few years from the occurrence of the 2001 mainshock, the effective permeability of the causative fault did not influence the permeability of the adjacent crustal blocks. This model gets further support from the inferences made by Sheldon and Micklethwaite (2007), where they suggested that after some lapse time the causative fault of any mainshock can enter into a healing regime and, thus, can become less permeable than the surrounding. Thus, the relatively smaller estimated diffusivity (i.e., smaller permeability) values are

possible in the lower crust underlying the Kachchh rift zone (Mandal 2012).

The local tomographic experiments revealed low and high-velocity patches on the causative fault of the 2001 mainshock (Mandal and Pujol 2006; Mandal and Chadha 2008). The low velocity patches at 0–10 km depths have been attributed to the meteoric water flow while deeper metamorphic fluid/volatile CO<sub>2</sub> (emanating from the carbonate melt pockets in the upper mantle (Mandal 2012)) flows mechanism have been used to explain low-velocity zones at 10–40 km depths. Further, support for this fluid flow model comes from the presence of dilatancy induced anisotropy resulting from microcracking and high pore fluid pressures in the epicentral zone of the 2001 mainshock, as revealed by the crustal shear-wave splitting study (Padhy and Crampin 2006; Mandal 2009b). This kind of crustal anisotropy has been observed for the rift zones in Iceland, where deep fluid circulation has been playing a key role in generating earthquakes (Crampin *et al.* 2002). Further, the deep electrical imaging of the KSZ has mapped several higher conductivity zones (fluid saturated) in the deep crust (at  $\geq 20$  km depths) below the main rupture zone of the 2001 Bhuj mainshock. Thus, the above findings can provide strong support for the model for deeper fluid circulation in the KSZ.

The presented results suggest that the observed spatio-temporal migration of seismicity (during 2001–2013) in the KSZ is consistent with the fluid flow and pore-pressure relaxation (caused by post-seismic stress changes induced by earthquakes) along the causative fault of the 2001 Bhuj mainshock. This model gets further support from the evidence of inferred shallow and deep fluid circulation and CO<sub>2</sub> degassing in the KSZ (Rodkin and Mandal 2012). We propose that the spatial and temporal pattern of the 2001 Bhuj earthquake sequence is controlled by the meteoric water flow in the upper crust (0–10 km depth) and deep metamorphic fluid/volatile CO<sub>2</sub> flow in the lower crust (10–40 km depths) below the KSZ. Thus, our results provide additional support for the key role played by deep fluid circulation in generating aftershock sequence of large intraplate earthquakes associated with continental rift zones.

### Acknowledgements

The authors are grateful to the Director, NGRI, for the support and permission to publish this work. The Ministry of Earth Sciences (MoES), New Delhi and CSIR–NGRI, Hyderabad (under the Heart Project) supported this work.

## References

- Antolik M and Dreger D S 2003 Rupture process of the 26 January 2001  $M_w$  7.6 Bhuj, India, earthquake from teleseismic broadband data; *Bull. Seismol. Soc. Am.* **93** 1235–1248.
- Antonoli A, Chiaraluce L, Cocco M and Piccinini D 2005 Fluid flow and seismicity pattern: Evidence from the 1997 Umbria–Marche (central Italy) seismic sequence; *Geophys. Res. Lett.* **32** L13011.
- Biswas S K 1987 Regional framework, structure and evolution of the western marginal basins of India; *Tectonophysics*. **135** 302–327.
- Biswas S K 2005 A review of structure and tectonics of Kutch Basin, western India, with special reference to earthquake; *Curr. Sci.* **88**(10) 15–30.
- Chung W Y and Gao H 1995 Source parameters of the Anjar earthquake of July 21, 1956, India and its seismotectonic implications for the Kutch rift basin; *Tectonophysics*. **242** 281–292.
- Courtillot V, Besse J, Vandamme D, Montigny R, Jaeger J J and Cappetta H 1986 Deccan flood basalts at the Cretaceous/Tertiary boundary? *Earth Planet. Sci. Lett.* **80** 361–374.
- Crampin S, Volti T, Chastin S, Gudmundsson A and Stefansson R 2002 Indication of high pore-fluid pressures in a seismically-active fault zone; *Geophys. J. Int.* **151** F1–F5.
- Gangopadhyay A and Talwani P 2003 Symptomatic features of intraplate earthquakes; *Seismol. Res. Lett.* **74**(6) 863–883.
- Gliko A 2011 *Potential seismic sources and seismic precursors – the base for real earthquake prediction*; (ed.) Gliko A O, Moscow 2011 (in Russian).
- Got J L, Frechet J and Klein F W 1994 Deep fault plane geometry inferred from multiplet relative relocation beneath the south flank of Kilauea; *J. Geophys. Res.* **99** 15,375–15,386.
- Gudmundsson A 2000 Active fault zones and groundwater flow; *Geophys. Res. Lett.* **27**(18) 2993–2996.
- Gupta H K, Harinarayana T, Kousalya M, Mishra D C, Mohan I, Rao N P, Raju P S, Rastogi B K, Reddy P R and Sarkar D 2001 Bhuj earthquake of 26 January 2001; *J. Geol. Soc. India* **57** 275–278.
- Havskov J and Ottemoller L 2003 SEISAN: The earthquake analysis softwares for Windows, Solaris and Linux, Version 8.0; Institute of Solid Earth Physics, University of Bergen, Norway, 400p.
- Kayal J R, Zhao D, Mishra O P, De R and Singh O P 2002 The 2001 Bhuj earthquake: Tomographic evidence for fluids at the hypocentre and its implications for rupture nucleation; *Geophys. Res. Lett.* **29** 5–4.
- Mandal P 2007 Sediment thicknesses and  $Q_s$  vs.  $Q_p$  relations in the Kachchh rift basin, Gujarat, India using Sp converted phases; *Pure. Appl. Geophys.* **164** 135–160.
- Mandal P 2009a Estimation of static stress changes after the 2001 Bhuj earthquake: Implications towards the Northward spatial migration of the seismic activity in Kachchh, Gujarat; *J. Geol. Soc. India* **74** 487–497.
- Mandal P 2009b Crustal shear wave splitting in the Epicentral Zone of the 2001  $M_w$  7.7 Bhuj Earthquake, Gujarat, India; *J. Geodyn.* **47** 246–258.
- Mandal P 2012 Passive source seismic imaging of the crust and upper mantle beneath the 2001  $M_w$  7.7 Bhuj earthquake region, Gujarat, India; *Bull. Seismol. Soc. Am.* **102**(1) 252–266.
- Mandal P and Chadha R K 2008 Three-dimensional velocity imaging of the Kachchh seismic zone, Gujarat, India; *Tectonophysics*. **452** 1–16.
- Mandal P and Horton S 2007 Relocation of aftershocks, focal mechanisms and stress inversion: Implications toward the seismotectonics of the causative fault zone of  $M_w$  7.6 2001 Bhuj earthquake (India); *Tectonophysics*. **429** 61–78.
- Mandal P and Pandey O P 2010 Relocation of aftershocks of the 2001 Bhuj earthquake: A new insight into seismotectonics of the Kachchh seismic zone, Gujarat, India; *J. Geodyn.* **49** 254–260.
- Mandal P and Pujol J 2006 Seismic imaging of the aftershock zone of the 2001  $M_w$  7.7 Bhuj earthquake, India; *Geophys. Res. Lett.* **33** L05309 1–4.
- Mandal P, Rastogi B K, Satyanarayana H V S and Kousalya M 2004 Results from local earthquake velocity tomography: Implications toward the source process involved in generating the 2001 Bhuj Earthquake in the lower crust beneath Kachchh (India); *Bull. Seismol. Soc. Am.* **94**(2) 633–649.
- Mandal P, Narsaiah R, Sairam B, Satyamurty C and Raju I P 2006 Relocation of early and late aftershocks of the 2001 Bhuj earthquake using joint hypocentral determination (JHD) technique: Implication toward the continued aftershock activity for more than four years; *Pure Appl. Geophys.* **163** 1561–1581.
- Mandal P, Chadha R K, Raju I P, Kumar N, Satyamurthy C, Narsaiah R and Maji A 2007 Coulomb static stress variations in the Kachchh, Gujarat, India: Implications for the occurrences of two recent earthquakes ( $M_w$  5.6) in the 2001 Bhuj earthquake region; *Geophys. J. Int.* **169** 281–285.
- Manning C E and Ingebritsen S E 1999 Permeability of the continental crust: Implications of geothermal data and metamorphic systems; *Rev. Geophys.* **37**(1) 127–150.
- McCalpin J P and Thakkar M G 2003 2001 Bhuj–Kachchh earthquake: Surface faulting and its relation with neotectonics and regional structures, Gujarat, western India; *Ann. Geophys.-Italy* **46**(5) 937–956.
- Miller S A, Collettini C, Chiaraluce L, Cocco M, Barchi M, Boris J and Kraus P 2004 Aftershocks driven by a high-pressure  $CO_2$  source at depth; *Nature* **427** 724–727.
- Mishra O P and Zhao D 2003 Crack density, saturation rate and porosity at the 2001 Bhuj, India, earthquake hypocentre: A fluid-driven earthquake; *Earth Planet. Sci. Lett.* **212** 393–405.
- Negishi H, Mori J, Sato H, Singh R P and Kumar S 2001 Aftershocks and slip distribution of mainshock: A comprehensive survey of the 26 January 2001 earthquake ( $M_w$  7.7) in the state of Gujarat, India; Research Report on Natural Disasters, December 2001, pp. 33–45.
- Noir J, Jacques E, Bekri S, Adler P M, Tapponier P and King G C P 1997 Fluid flow triggered migration of events in the 1989 Dobi earthquake sequence of central Afar; *Geophys. Res. Lett.* **24** 2335–2338.
- Nur A and Booker J R 1972 Aftershocks caused by pore fluid flow? *Science* **175** 885–887.
- Padhy S and Crampin S 2006 High pore-fluid pressures at Bhuj, inferred from  $90^\circ$ -flips in shear-wave polarizations; *Geophys. J. Int.* **164** 370–376.
- Poupinet G, Ellsworth W L and Frechet J 1984 Monitoring velocity variations in the crust using earthquake doublets: An application to the Calaveras fault, California; *J. Geophys. Res.* **89** 5719–5731.
- Pujol J 1988 Comments on the joint determination of hypocentres and station corrections; *Bull. Seismol. Soc. Am.* **78** 1179–1189.
- Rastogi B K, Aggrawal S K, Rao N and Choudhury P 2013 Triggered/migrated seismicity due to the 2001  $M_w$  7.6

- Bhuj earthquake, western India; *Natural Hazards* **65**(2) 1085–1107.
- Rodkin M and Mandal P 2012 A possible physical mechanism for the unusually long sequence of seismic activity following the 2001 Bhuj  $M_w$  7.7 earthquake, Gujarat, India; *Tectonophysics*. **536/537** 101–109.
- Sarkar D, Sain K, Reddy P R, Catchings R D and Mooney W D 2007 Seismic – reflection images of the crust beneath the 2001  $M=7.7$  Kutch (Bhuj) epicentral region, western India; *Geol. Soc. Am. Spec. Paper* **425** 319–327.
- Shapiro S A, Audigane P and Royer J J 1999 Large scale *in situ* permeability tensor of rocks from induced microseismicity; *Geophys. J. Int.* **137** 207–213.
- Shapiro S A, Patzig R, Rothert E and Rindshwentner J 2003 Triggering of seismicity by pore-pressure perturbations: Permeability-related signature of the phenomenon; *Pure Appl. Geophys.* **160** 1051–1066.
- Sheldon H and Micklethwaite S 2007 Damage and permeability around faults: Implications for mineralization; *Geology* **35**(10) 903–906.
- Talwani P and Acree S 1984 Pore-pressure diffusion and the mechanism of reservoir-induced seismicity; *Pure Appl. Geophys.* **6** 947–965.
- To A, Burgmann R and Pollitz F 2006 Post-seismic deformation and stress changes following the 1819 Rann of Kachchh, India earthquake: Was the 2001 Bhuj earthquake a triggered event? *Geophys. Res. Lett.* **31** L13609, 1–4.

*MS received 31 August 2015; revised 19 March 2016; accepted 6 June 2016*

Corresponding editor: PAWAN DEWANGAN